Physics 335 project report

Testing CsI scintillators with cosmic muons.

Rhys G. Povey

(Dated: May 20, 2012)

MUONS APPEARED OUT OF THE SKY AND RAINED DOWN UPON THE CRYSTAL SCINTILLATORS. MADNESS ENSUED.

I. INTRODUCTION

Caesium iodide (CsI) is a high performance crystal scintillator. The new CPV kaon decay experiment, k0TO, under construction in Japan [1] will be using 2576 CsI crystals to form the calorimeter. Combined with newly developed electronics, these CsI scintillators are designed to exhibit a time resolution on the order of 100 ps. In an effort to precisely measure charge-parity violating effects in the standard model, k0TO will be studying the rare kaon decay $K_L^0 \to \pi^0 \nu \overline{\nu}$. To test the performance of the CsI scintillators a set of 16 were used in a cosmic muon stack detector.

A. Charge parity violation

Within the standard model of particle physics, the weak interaction mediates flavour changing processes and the Cabibbo-Kobayashi-Maskawa (CKM) matrix describes the relationship between mass eigenstates and weak interaction eigenstates [2, 3]. The existence of small complex components in the CKM matrix allows charge-parity (CP) conservation to be violated. These effects can be theoretically calculated and experimental measurements on CP violating (CPV) events provides a stringent test of the standard model (SM).

One particular CPV event of note is the rare long kaon decay into a pion and neutrinos, $K_L^0 \to \pi^0 \nu \overline{\nu}$. This is a direct CP violating process and decays through a loop, making it one of the most sensitive probes to CPV in the quark sector [4]. The branching ratio can be predicted by SM calculations relatively accurately to $(2.84 \pm 0.4) \times 10^{-11}$. Whilst very small and difficult to measure, this event provides a good test of the standard model and any new physics in the quark CPV sector. Experimentally, the event is detected by the decay of the π^0 to 2 photons.

B. K0TO, J-PARC E-14

Experiment 14 at the Japan Proton Accelerator Research Complex (J-PARC) in Tokai [1], is the latest experiment to measure kaon decays. Now named K0TO (K^0 at Tokai), the experimental goal is to determine the branching ratio of $K_L^0 \to \pi^0 \nu \overline{\nu}$. K0TO is the direct successor to E319a, the first experiment dedicated to this decay mode, which provides the current upper limit on the branching ratio at 2.6×10^{-8} [5]. This achievement follows from a long series of kaon decay experiments with improving sensitivities [6–11].

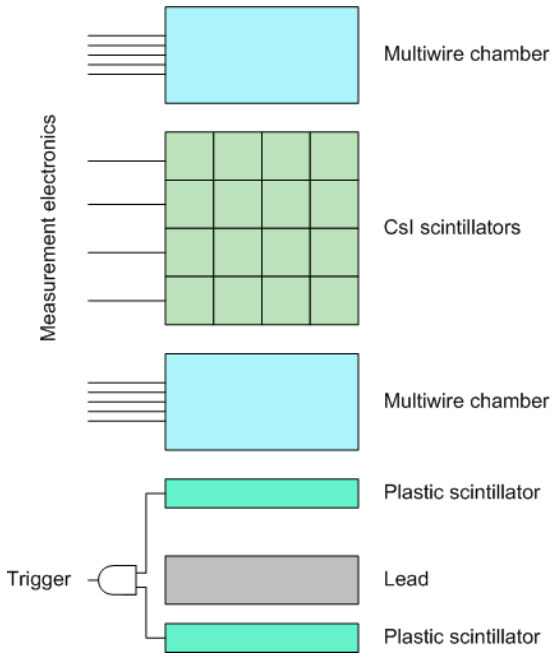

FIG. 1. Drawing of the cosmic muon stack detector.

The K0TO experiment is a collaboration between 16 institutions and has been in the works since the 2006. Beam tests started in early 2012 and preliminary runs are scheduled for later in the year. Full operation is planned to begin in 2013. Part of the upgrade to K0TO is a new calorimeter of CsI crystals originally from kTeV. A new data acquisition system with custom built electronics is also being employed to maximize the performance of the CsI scintillators.

C. Muon stack detector

To test the CsI scintillators and measurement electronics, a cosmic muon stack detector has been constructed at the University of Chicago. Cosmic muons are in abundance and make a good test particle for detection. The detector, pictured in Fig. 1, consists of three main parts: plastic scintillators for a trigger system, wire chambers for track determination, and the CsI scintillators. Each of these parts is connected to the data acquisition system. In this report we describe the experimental apparatus,

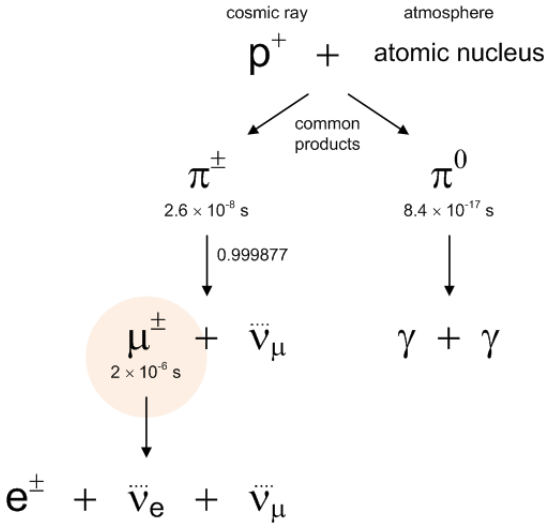

FIG. 2. Diagram depicting decay chain from cosmic ray to cosmic muon.

measurement electronics, and data analysis.

II. THE EXPERIMENT

A. Cosmic muons

Cosmic muons are produced in the upper atmosphere by incoming highly energetic protons (cosmic rays). These protons collide with atomic nuclei and commonly produce pions. Positive and negative pions then have 0.999877 branching ratio decay into muons, $\pi^- \to \mu^- \overline{\nu}_\mu$ or $\pi^+ \to \mu^+ \nu_\mu$. Muons have a mean lifetime of $2\,\mu$s allowing those with energies $\gtrsim 1\,$GeV to reach the surface. Figure 2 summarizes the process of cosmic ray to cosmic muon. For our experiment we expect the flux of cosmic muons passing through the detector to be in the order of a Hz.

B. Trigger system

The trigger system is located on the bottom of the stack and consists of two flat plastic scintillators. The scintillators are separated vertically by $\approx 1\,$m with 10 cm worth of lead in between. Vertical separation limits the triggering particles to those coming down vertically and the lead eliminates any low energy charged particle background. In the horizontal plane the scintillators measure approximately $60\,\text{cm} \times 40\,\text{cm}$, covering an area over twice that of the CsI crystals.

Each scintillator is hooked up to a discriminator (LeCroy model 821 quad discriminator) that fires a 100 ns NIM logic pulse whenever it receives a signal over 60 mV. These are fed into an and-gate (LeCroy model 364 4-fold logic gate) that outputs a NIM logical signal whenever the inputs overlap. The trigger signal is then sent through a NIM-ECL and ECL-LVDS converter. Finally, the LVDS logic trigger is input to the top level MT (master time) board, which handles distribution. A diagram of this process is given in Fig. 3.

The trigger system was found to have a moderate accidental rate, with only half of the recorded data including hits on the CsI crystals. Given the relative areas of the scintillators, however, this was expected. A third plastic scintillator was originally part of the trigger system but was faulty and had to be removed.

C. Caesium iodide crystals

Sixteen CsI scintillators form the main the component of the muon stack detector. Each measures $5\,\text{cm} \times 5\,\text{cm} \times 50\,\text{cm}$, is wrapped in black plastic, and is attached to a photo-multiplier tube (PMT) with an ultraviolet filter. They are arranged in a 4×4 stack such that a muon coming down will strike four different crystals. The stack of CsI crystals and PMTs are housed in a light-tight box with nitrogen gas pumped through it. Caesium iodide is slightly hygroscopic (absorbs water from its environment) and thus the nitrogen gas is used to displace air which holds water molecules.

The 16 CsI channels are labeled 1 to 16 starting at the top and going across then down. Each CsI scintillators was run at 1400 V, and the signal output from the PMT was passed through a $50\,\Omega$ to differential converter and amplifier before reaching the data acquisition boards. During the final run of data taking the CsI scintillator on channel 2 was not working correctly.

D. Wire chambers

To determine the track the muon takes through the stack detector, two multi-wire chambers [12], positioned above and below the CsI crystals, were used. The wire chambers were assembled by undergraduate students the previous summer, they are boxes $40\,\text{cm} \times 40\,\text{cm}$ and 11 cm high. They are vertically separated (base to base) by 91 cm. Inside is 4 horizontal layers of wires, with 2 layers running in each perpendicular direction. Each layer has 18 wires, 8 of which are active with a high voltage (2150 V) and 10 of which are grounded, in a grounded-active-grounded sequence. Between the two layers running in the same direction, the relative positions of the active and grounded wires are offset by one. This configuration removes the left-right ambiguity inherent in a single layer of wires. The chamber is pumped with a mixture of argon and carbon dioxide gas, the argon is the ionizable material whilst the carbon dioxide is used to quench runaway ionizations.

A charged particle entering the wire chamber will ionize the gas as it passes and the ionized electrons will be attracted to the active wires, producing a signal when

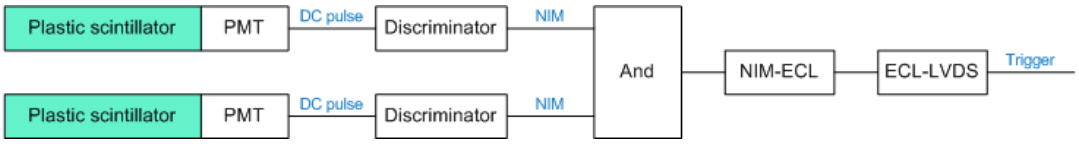

FIG. 3. The trigger system used for stack detector.

they hit. Ideally, a particle moving through vertically will signal one wire in each layer to give an accurate position measurement. Our wires are separated by 16 mm, so a two-layer arrangement with offset creates a 8 mm, i.e. ±4 mm, region for the particle's passing position. The produced signal is already differential and is only sent through an amplifier before the data acquisition boards. Each wire is given its own channel for data, and thus 64 channels are used by the full two wire chamber system. CAT-6 cables are particularly effective at transferring differential signals and were used here to connect the wire chambers to the measurement electronics some 5 m away.

Unfortunately, the area covered by the wire chambers does not cover the total area of the CsI crystals and the cross section for our experiment is limited to the overlap of around 20 cm × 25 cm in the horizontal plane. As the flux of cosmic muons is large this is not a problem and hits come on the order of 10 s. A computer graphic in Fig. 4 shows the relative positioning and scale of the wire chambers relative to the CsI crystals. A larger, and decades old, multi-wire chamber was originally intended for use above the CsI crystals and sits at the top of the stack structure. Problems with wire oscillations, charge build-ups, and shielding made it more problematic than it was worth, however.

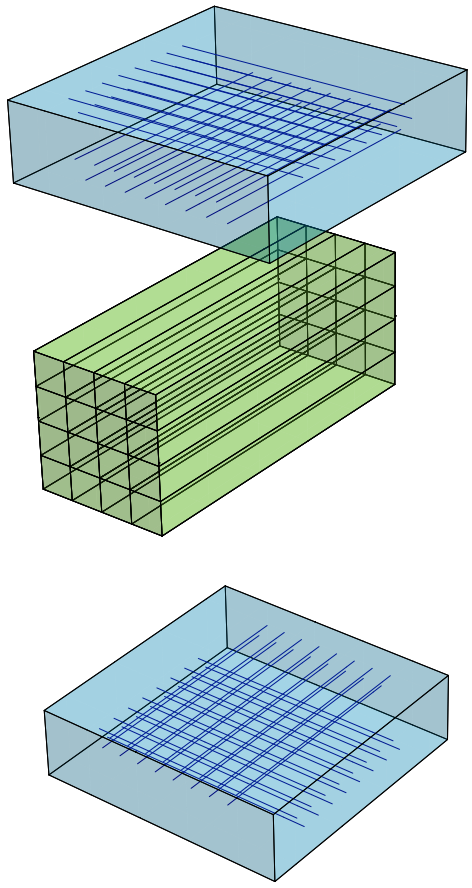

FIG. 4. Layout of the multi-wire chambers and CsI crystals. The 16 CsI crystals are in green and the wires are in blue.

E. Measurement electronics

A major part of this experiment is to test the new data acquisition system accompanying the CsI scintillators. Custom built as the University of Chicago, the analog to digital converter (ADC) boards that capture the incoming signals have Gaussian filter system built in. This filter transforms a traditional scintillator pulse (sharp rise and then decay) into a Gaussian pulse. The Gaussian pulse is then sampled every 8 ns (125 MHz) and saved to a linked computer. Finding the time the signal arrived can then be done by fitting a Gaussian to the data and locating the peak's position. This method provides a much easier and unambiguous way of determining signal times. Importantly, the signal can be resolved to much shorter times than the sampling time, as less points are needed to reconstruct the Gaussian pulse. The data values captured by the ADC are simply given in 'counts' proportional to voltage, with the area under the Gaussian proportional to energy, such that the highest energy particles picked up in K0TO won't overflow the allocated memory.

Each ADC board takes 16 channels, and thus 5 boards were needed for this experiment. To synchronize the data taking, master time (MT) boards are used to distribute a clock and trigger signal. Each MT board has 8 outputs of clock plus trigger. The output of the trigger system is fed into a 'top-level' MT board which uses an on board oscillator as the master clock. Two outputs are then used to go to 'second level' MT boards. From these two boards the clock and trigger is then distributed to the ADC boards. This 2 level system was implemented in case more than 8 ADC boards were needed, as would have been the case if the large multi-wire chamber was used. A simple diagram of the setup is given in Fig. 5. The ADC board are plugged into a crate that connects

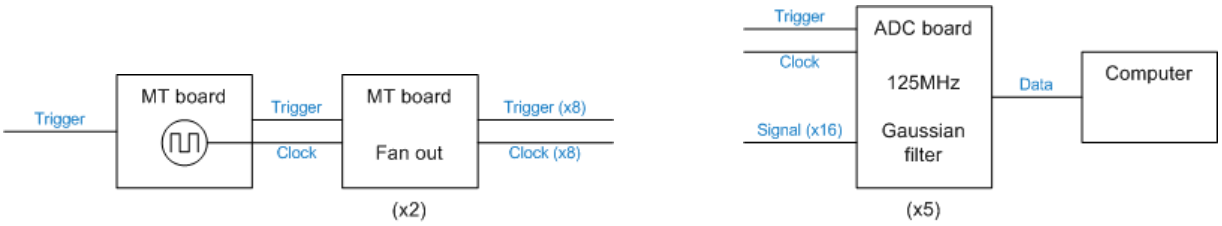

FIG. 5. The data acquisition system.

them to a computer which controls the boards and stores the data.

F. Operation

To start the data taking process a previously written script is executed on the crate computer from a remote terminal. For each trigger signal, the ADC boards take 200 samples of data (over 1592 ns). After 20 events the on board memory of the ADC boards fill up and data taking temporarily stops as everything is sent to the crate computer. A data file is then written on the computer containing 12 boards $\times$ 20 events $\times$ 200 samples. Only 5 board had anything plugged into them, however.

Several iterative runs of the experiment were made with varying numbers of boards used and equipment attached, Initially only 96 samples were taken per event, and 40 events per readout, but the wire chamber signals are sometimes delayed and 200 samples was found to be a safer window for capturing everything. The final data run which is presented here was taken on the 2nd of May 2012 and includes 10,000 triggered events.

III. DATA ANALYSIS

A. Pedestal subtraction

The first step to analyzing the data is pedestal subtraction. The background voltages on the various channels is generally not zero and this 'pedestal' value needs to be subtracted to fit Gaussians and compare channels. As each event only registers on a handful of channels, or often on none, there is a wealth of pedestal information in the acquired data.

Obtaining the pedestals was done by looking over the first 600 events. For a particular channel, the total standard deviation from each event was calculated. Then the mean and standard deviation of this list was found. Events with a standard deviation within 1σ of the mean standard deviation were chosen as null events with no signal. Now, the mean value of the data from each null event is calculated, and the mean of this is taken as the pedestal value. The standard deviation of these means was also computed. Lastly, the mean of standard deviations from the null events, denoted threshold-σ, was calculated to be used when determining if the channel received a hit. This process is carried for each of the 80 channels.

4	3	2	1
8	7	6	5
12	11	10	9
16	15	14	13

FIG. 6. CsI channel hits from event 2 (scintillators recording a hit are shaded green).

Typical pedestal levels (mean of means) were between 250 and 350 counts. For the CsI scintillators the pedestal standard deviation (standard deviation of means) was around 0.7 ± 0.1, and the threshold-σ (mean of standard deviations) was between 2 and 3. For the wires the pedestal standard deviation and threshold-σ was higher, both ranging from 3 to 12.

B. Hit determination

When analyzing an event, the first operation is a check to see which channels registered a hit. For each channel, a hit was recorded on the condition that the maximum data value was greater than 10 threshold-σ for that channel. By tabulating the hit channels for each event we can choose subsets of events to further analyze. We expect a muon traveling through the CsI crystal stack to cause 4 crystals in a column to scintillate, or more depending on the angle of approach. A wide variety of event types were recorded: some as expected, some with only a few stray wire hits, some completely null, some with CsI hits but only a couple of wires, some with more than 4 CsI hits, and a few where everything hit. Many of these are from triggers when the muon didn't pass through the CsI, the presence of other charged particles, or showering events. A sample hit pattern is given in Fig. 6.

The events we are most interested in are those hitting exactly 4 CsI crystals in a column and hitting enough wires that the track can be reconstructed, i.e. at least one

CsI column	Hits	Good events
1, 5, 9, 13	402	4
6, 10, 14	447	14
3, 7, 11, 15	509	102
4, 8, 12, 16	476	21
Total	1834	141

TABLE I. Number of single column only and 'good' events the CsI scintillators. Good events have a reconstructible track through the column of CsI crystals and do not hit any other crystals.

wire in each direction in both the top and bottom wire chamber. Of the 10,000 triggers, 141 events were found to satisfy these conditions with a break down given in Tab. I. The inhomogeneous efficiency of the wire chamber, particularly around the edge, gives a non uniform sample of good events.

C. Gaussian fitting

If a CsI channel is flagged as hit, we can fit a Gaussian to the data and extract the pulse timing. As neither the Gaussian filters or incoming scintillator pulses are perfect, the ADC output is not perfectly Gaussian. There is a generally slight asymmetry in the peak with slower decay in positive time direction. To account for this, a higher order generalized Gaussian is fit instead. The fit function is

$$f(t) = A\exp\left(-\frac{1}{2}\left(\frac{t-\mu}{\sigma}\right)^2 - \alpha\left(\frac{t-\mu}{\sigma}\right)^3 - \beta\left(\frac{t-\mu}{\sigma}\right)^4\right), \tag{1}$$

with 5 parameters: A, μ, σ, α, β. Accurate determination of the pedestal (Sec. III A) removes the need to fit a vertical shift constant.

To generate a good fit quickly, we need estimates for the parameters A, μ, and σ. To find these we first do a standard Gaussian fit of the form

$$f_1(t) = A\exp\left(-\frac{1}{2}\left(\frac{t-\mu}{\sigma}\right)^2\right),$$

with 3 parameters: A, μ, σ. Initial estimates of A and μ are made by finding the maximum value data point. From fit f, Eq. (1), we can find the peak position (in time), μ. The uncertainty, $\Delta\mu$, is taken from the standard fit error for μ. Figure 7 gives some typical CsI scintillator data and the fitted Gaussian.

This fitting is done only for the CsI scintillator channels. We are not concerned with the timing on the wire channels, only their hit status. In theory it would be possible to analyze the wire timings, thereby using it as a drift chamber, where the delay gave information on how far from the wire the muon passed. This adds another level of complication to the experiment, however, for only a small unneeded refinement in position accuracy.

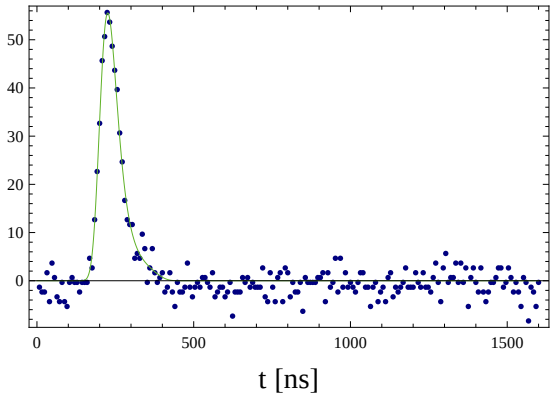

FIG. 7. CsI channel 7 data from event 2 with Gaussian fit curve in green. Here $\mu = 225.848\,\text{ns}$ and $\Delta\mu = 0.989\,\text{ns}$.

At this point in the analysis the peak times from different CsI scintillators are unrelated as there is no timing reference point or calibration between the crystals. Ideally a controlled pulse source, such as a laser, could be used to flash all the crystals simultaneously and deduce the relative timing offsets between the CsI channels. Unfortunately, access to such a tool was not available. In Sec. III E and Sec. III F some post-data calibration methods are attempted.

D. Track reconstruction

The track of the muon through the stack detector is determined by the two wire chambers. For a track to be reconstructed there must be a signal in at least one wire in each direction in both the top and bottom chambers. Whilst in principle we expect 8 wires to be hit (1 in each layer of wires), the multi-wire chamber is not as reliable as the CsI crystals and this is rarely the case. The track is created by joining a line between a point in the top wire chamber and a point in the bottom wire chamber.

The connecting point in each wire chamber has 3 coordinates: x, y in the horizontal plane, and z vertically. First we take the collection of hit wires running parallel to $\vec{y}$ in both layers, each having a x and z coordinate, and take the mean x and z values. Second we do the same thing to wires parallel to $\vec{x}$, each with a y and z coordinate, to get a mean y and z value. Lastly we combine these two pairs, taking the mean z, to get a final (x, y, z) position. This process is done separately for both the top and bottom wire chamber.

The uncertainty in the horizontal position of these points (and hence the track) is estimated to be around 8 mm, ± 4 mm from the resolution of the wire chamber (Sec. II D) and another ± 4 mm from determining the position of the wire chamber relative to the CsI crystals. As the vertical separation between the boxes is just under

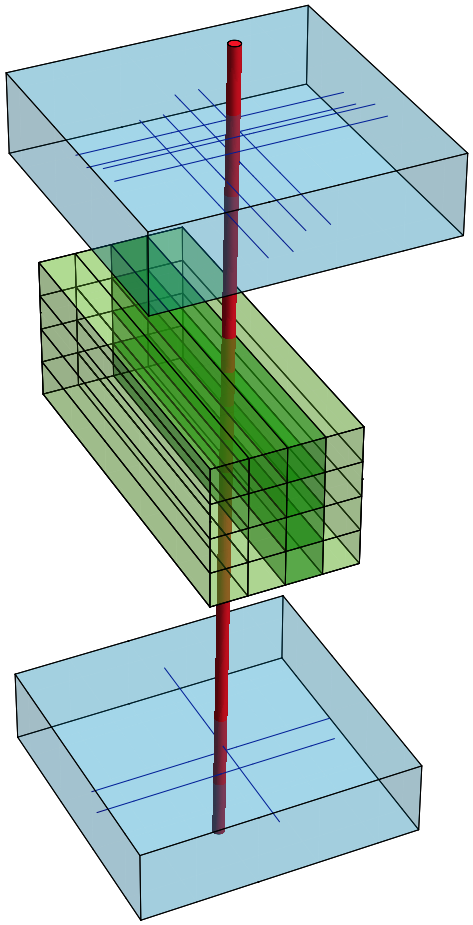

FIG. 8. Track reconstruction for event 272. The hit CsI crystals are highlighted in dark green, whilst the hit wires are drawn in blue. A red cylinder, with radius representing uncertainty, shows the path the muon took through the stack detector.

1 m, small deviations in the top and bottom coordinates do not significantly affect the track angle. A sample track reconstruction is shown in Fig. 8.

E. CsI timing calibration by tracks

Knowing the muon tracks through the stack detector we can determine where each CsI crystal was hit and, assuming the muon travels at approximately c, we can infer when it should have hit as well. Cosmic muons picked up by our stack detector have energies $\gtrapprox 2\,\text{GeV}$ (picked out by the lead) and muons have a rest mass of $\approx 100\,\text{MeV}$, thus $v/c \gtrapprox 0.999c$. Calibrations with this technique is done on each column separately using 'good' events with single column CsI hits and enough wire hits for reconstruction as selected in Sec. III B and Tab. I. There is no information on relative timings between different columns. Only the timing difference between scintillators can be extracted and thus we arbitrarily use the top CsI crystal as the reference point for each column.

The calibration process is done as follows. For each column we take the set of good events which we can analyze. Then, for each event we calculate some time offsets between the top CsI scintillator and the others. Lastly, we combine the results from different events. For a set of 4 Csi scintillators, there are 6 ($^4C_2$) difference times, and we can combine them together to get a self-consistent averaged result for the 3 offsets we want in each event.

To walk through this process we will consider the CsI column of $1, 5, 9, 13$, and one particular event hitting these crystals. Using the wire chamber data we obtainaa track that parameterizes x and y in terms of vertical position z, $(x(z), y(z), z)$. Then, for each CsI crystal we used the middle vertical distance to define a point, $\vec{r}$, that the muon hit, i.e.

$$\vec{r}_1 = \begin{pmatrix} x(175\,\text{mm}) \\ y(175\,\text{mm}) \\ 175\,\text{mm} \end{pmatrix} \qquad \vec{r}_5 = \begin{pmatrix} x(125\,\text{mm}) \\ y(125\,\text{mm}) \\ 125\,\text{mm} \end{pmatrix}$$
$$\vec{r}_9 = \begin{pmatrix} x(75\,\text{mm}) \\ y(75\,\text{mm}) \\ 75\,\text{mm} \end{pmatrix} \qquad \vec{r}_{13} = \begin{pmatrix} x(25\,\text{mm}) \\ y(25\,\text{mm}) \\ 25\,\text{mm} \end{pmatrix} .$$

The functions $x(z), y(z)$ include uncertainties from the track finding. The time difference that should be measured between two CsI scintillators is equal to the muon flight time between crystals plus the extra scintillated photon travel time from a non-vertical track. Thus for CsI crystals a and b, extending toward the PMT in the y direction,

$$\Delta t_{a,b} = t_a - t_b = \frac{y_a - y_b}{c/n} - \frac{|\vec{r}_a - \vec{r}_b|}{c} ,$$

where $n = 1.739$ is the index of refraction for caesium iodide.

Now, if $\Delta m_{a,b} = \mu_a - \mu_b$ is the measured time difference between CsI scintillators a and b, then

$$\Delta m_{a,b} = \Delta t_{a,b} + \Theta_{a,b} , \tag{2}$$

where $\Theta_{a,b}$ is the systematic time offset. Note that $\Theta_{a,b} = -\Theta_{b,a}$. So for our cosmic muon event, we can extract 6 offsets:

$$\Theta_{1,5},\ \Theta_{1,9},\ \Theta_{1,13},\ \Theta_{5,9},\ \Theta_{5,13},\ \Theta_{9,13} .$$

Although we have 6 time offsets, we only need 3 to describe our system. The other 3 can be written as linear combinations of these; it should hold that $\Theta_{a,c} = \Theta_{a,b} + \Theta_{b,c}$. Arbitrarily we choose the top CsI crystal as our reference and thus the offsets $\Theta_{1,5}, \Theta_{1,9}, \Theta_{1,13}$. We still

want to use the other 3 pieces of information, however, and so we define averaged offsets, $\Phi_{1,5}, \Phi_{1,9}, \Phi_{1,13}$, that simultaneously satisfy the equations

$$\begin{aligned} \Phi_{1,5} &= \Theta_{1,5} \ , \\ \Phi_{1,9} &= \Theta_{1,9} \ , \\ \Phi_{1,13} &= \Theta_{1,13} \ , \\ \Phi_{1,9} - \Phi_{1,5} &= \Theta_{5,9} \ , \\ \Phi_{1,13} - \Phi_{1,5} &= \Theta_{5,13} \ , \\ \Phi_{1,13} - \Phi_{1,9} &= \Theta_{9,13} \ . \end{aligned} \tag{3}$$

We can think of this system of equations as defining planes in $\mathbb{R}^3$ with basis vectors $\widehat{\Phi}_{1,5}, \widehat{\Phi}_{1,9}, \widehat{\Phi}_{1,13}$. Hence, our goal is determine the point

$$\begin{pmatrix} \Phi_{1,5} \\ \Phi_{1,9} \\ \Phi_{1,13} \end{pmatrix} \in \mathbb{R}^3$$

that best satisfies the intersection of planes described by Eqs. (3). The 6 difference relationships between the 4 CsI scintillators and the plane equations they produce can be visualized graphically as in Fig. 9.

To make this 3 dimensional fit our approach is to reduce the problem to 3 one dimensional fits. Starting with our set of 6 planes, we take every pair combination and intersect them to get a line. This gives us a set of ${}^6C_2 = 15$ lines in $\mathbb{R}^3$, reducing the problem of intersecting planes to intersecting lines. Now, from this set of lines we again take every pair combination. As these lines exist in $\mathbb{R}^3$ they do not necessarily intersect, thus we instead find their closest approach and take the midway point. Finally we obtain a set ${}^{15}C_2 = 105$ points in $\mathbb{R}^3$. This process of intersecting planes to form lines carries the uncertainties from the track position in the standard way for operations of multiplication and addition. When getting the midway point between 2 lines, the closest approach point on each line carries a different uncertainty and the midway point is obtained by making a fit to these points weighted by their uncertainty. A sample of the lines produced by intersecting planes is shown in Fig. 10.

With the problem is this form, we can now separate components and fit for the 3 averaged offsets separately. Each of $\Phi_{1,5}, \Phi_{1,9}, \Phi_{1,13}$ is determined by fitting to 105 values weighted by their uncertainty. After obtaining these 3 offsets for each event in a CsI column set, they can be combined to give a final result for the time difference offsets in the experiment. This is again done by fitting weighted to uncertainties. Sample final fits are given in Fig. 11, and the full set of time difference offset results are given in Tab. II.

For the CsI column of channels 6, 10, 14, there is only 3 CsI scintillators and thus only 3 time difference connections between them. In this case we make 2 basis connections and solve the problem of ${}^3C_2 = 3$ lines intersecting in $\mathbb{R}^2$.

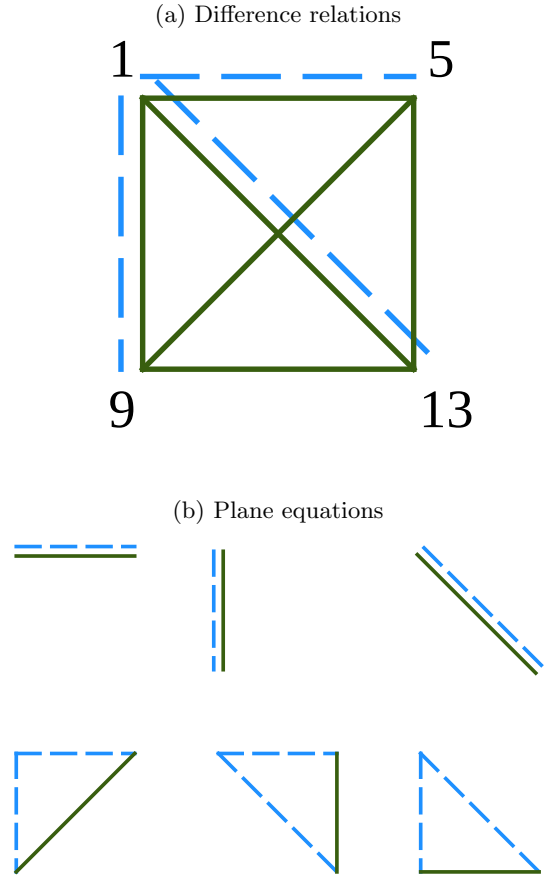

FIG. 9. Graph representation of the 6 difference relations from 4 CsI scintillators and the plane equations they describe. (a) Each CsI channel is given a node and 6 connections (green) $\Theta_{a,b}$, representing time offsets, can be made between them. The dashed blue lines are the connections we choose to be the basis $\Phi_{a,b}$. (b) Using the basis connections, each time difference connection can be made into a loop that then defines a plane. For example, the top left graph states that $\Theta_{1,5} + \Phi_{5,1} = \Theta_{1,5} - \Phi_{1,5} = 0$, and the bottom right graph states that $\Theta_{9,13} + \Phi_{13,1} + \Phi_{1,9} = \Theta_{9,13} - \Phi_{1,13} + \Phi_{1,9} = 0$. These give Eqs. (3).

$\Phi_{1,5}$	-1.449 ± 0.814 ns
$\Phi_{1,9}$	4.422 ± 0.892 ns
$\Phi_{1,13}$	3.561 ± 0.603 ns
$\Phi_{6,10}$	4.324 ± 0.298 ns
$\Phi_{6,14}$	13.437 ± 0.266 ns
$\Phi_{3,7}$	1.556 ± 0.082 ns
$\Phi_{3,11}$	6.212 ± 0.100 ns
$\Phi_{3,15}$	1.865 ± 0.060 ns
$\Phi_{4,8}$	0.957 ± 0.182 ns
$\Phi_{4,12}$	5.695 ± 0.207 ns
$\Phi_{4,16}$	8.472 ± 0.213 ns

TABLE II. Time difference offsets between CsI scintillators using track reconstruction calibration.

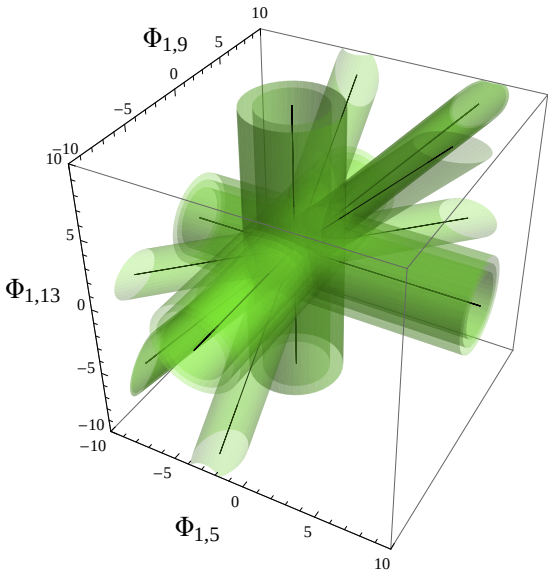

FIG. 10. Lines formed by intersection of time difference planes for event 4078. Cylinder radii represent uncertainties.

Event	Relative total energy
2128	104,819
3501	21,477
4945	266,431
9259	23,895

TABLE III. Candidate shower events with ≥ 14 CsI hits, and calculated relative total energies.

F. CsI timing calibration by showers

When particularly high energy cosmic rays collide with atomic nuclei in the atmosphere they can produce a shower of muons. A shower of muons hitting the stack detector will hit every CsI crystal and wire. If we assume these showers are sharp and clean such that they hit everything at the same time, we can use them to calibrate the channel timings.

Within our acquired data, 4 events, given in Tab. III, had 14 or more CsI crystal hits (the next highest amount was 11). Relative total energies were calculated by integrating under the Gaussian peaks and summing over the crystals. Of these 4 events, 2 had a total energy an order of magnitude above the other 2. These events, numbered 2128 and 4945, we identified as high energy shower events. Using the time difference of the CsI scintillators in these events an alternative calibration procedure was carried out.

For each shower event, the full set of time difference offsets, as described in Eq. (2) but now with

$$\Delta t_{a,b} = t_a - t_b = \frac{z_a - z_b}{c} \ ,$$

were found. As the shower events had different distributions of CsI channel hits, it is simplest to combine the events at this point and analyze a full set of ${}^{15}C_2 = 105$ connections, $\Theta_{a,b}$. Averaged offsets were found by fitting weighted to uncertainties.

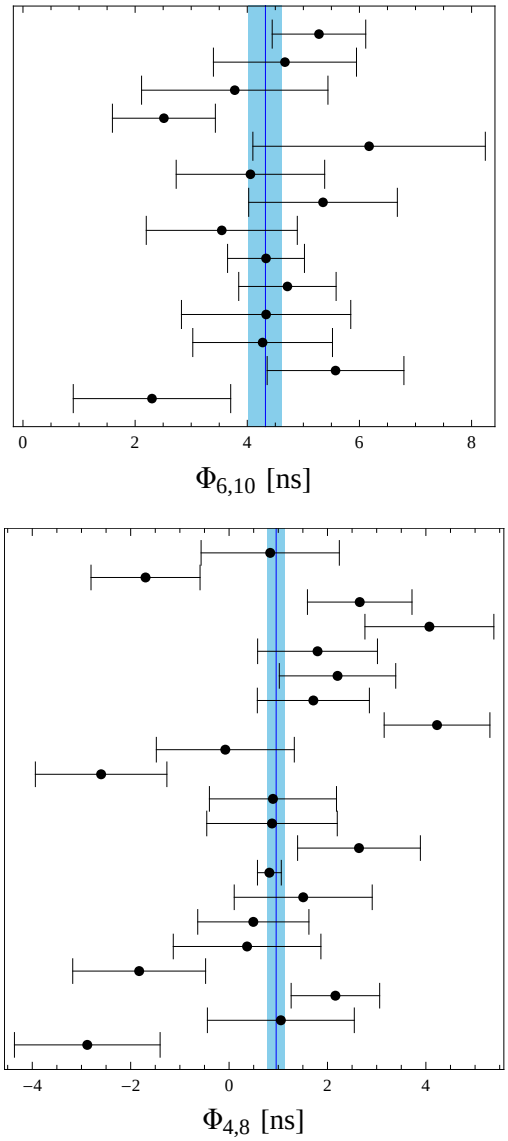

FIG. 11. Fits for time difference offsets $\Phi_{6,10}$ and $\Phi_{4,8}$ from the combination of appropriate column events. Each point in the plots comes from a different event. The blue line and light blue shading represent the fit value and uncertainty respectively. Uncertainties are drawn at 1σ levels.

Using the previous method of Sec. III E, we would need to start intersecting hyperplanes in $\mathbb{R}^{14}$. Instead, we break the set of offsets into subsets for each CsI column and discard offsets relating channels of two different columns. As the events we want to analyze only hit single columns we are not concerned with cross-column calibration. With more time and computation power, however, a full analysis on 105 connections could be made.

The 4 column subsets of time difference offsets are now analyzed independently, exactly as in Sec. III E by inter-

$\Phi_{1,5}$	-1.380 ± 0.184 ns
$\Phi_{1,9}$	3.011 ± 0.194 ns
$\Phi_{1,13}$	3.160 ± 0.133 ns
$\Phi_{6,10}$	1.826 ± 0.259 ns
$\Phi_{6,14}$	11.823 ± 0.221 ns
$\Phi_{3,7}$	1.475 ± 0.139 ns
$\Phi_{3,11}$	5.867 ± 0.099 ns
$\Phi_{3,15}$	1.376 ± 0.109 ns
$\Phi_{4,8}$	0.676 ± 0.144 ns
$\Phi_{4,12}$	5.152 ± 0.143 ns
$\Phi_{4,16}$	6.775 ± 0.132 ns

TABLE IV. Time difference offsets between CsI scintillators using shower events.

secting planes. Results from this calibration method are give in Tab. IV

IV. RESULTS

A. Sample events

One of the outcomes of this experiment was the ability to detect cosmic muons and their path through the stack detector. For good events through single CsI columns, we can calibrate them according to Eq. (2). If we define $t_{\text{top}} = \mu_{\text{top}}$, then

$$t_a = \mu_a - \Phi_{\text{top},a}\,.$$

For a muon descending vertically upon the apparatus, traveling at c, the bottom most CsI scintillator should fire ≈ 0.5 ns after the top CsI scintillator. This delay is often less than the timing uncertainty in the CsI scintillators.

A series of sample events from Tab. I are appended in Figs. 13, 14, 15, 16.

Glancing over the final results we can see there is a definite issue with CsI scintillator pulse arrival times. Whilst for many events the calibration correctly places them in order (within uncertainties), other events are clearly not firing in the expected sequence. It is impossible to discern whether these events are in fact muons, hitting the CsI crystals in the correct order, and there is a problem with the measurement; or whether they are not cosmic muons, but instead some background event. If they are muons, it is possible there some sort of neglected scattering process happening. The decay of muons into electrons within the detector is another possibility, although this should not set off the trigger through the lead. Multiple muons passing through the detector would also cause anomalous results but this should be extremely rare.

For the majority of events we can also see that the track calibration method seems to produce better results. This is expected, however, as its formulation is biased and uses the results to make the fit. Regardless, it is obvious there is an unaccounted for effect cause non-uniform shifting in the CsI scintillator timings relative to each other.

Event	CsI chan.	$\Delta\mu$
2128*	7	0.0988 ns
3844	14	0.0886 ns
4945*	11	0.0833 ns
5225	5	0.0871 ns

TABLE V. High energy and narrow time resolution CsI scintillator hits. Note that the two asterisked events are our shower events from Tab III.

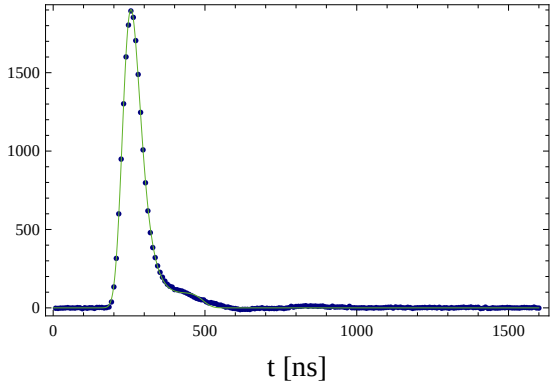

FIG. 12. CsI channel 11 data from event 4945 with Gaussian fit curve in green. Here $\mu = 256.195$ ns and $\Delta\mu = 0.083$ ns.

The K0TO experiment in Japan will typically be measuring photons with energies on the order of 100 GeV. Whilst the majority of cosmic muons are well below this level, high energy events as this level are not uncommon. Higher energetic particles are able to deposit more energy into the CsI scintillator and produce a larger pulse. The noise in measuring this pulse is constant. so the signal to noise ratio is much better for high energy particles. Thus when fitting Gaussians to high energy scintillations we get a better fit with smaller errors.

A simple search for the smallest fit errors in CsI scintillator hits reveals the high energy cosmic muon events, as well as the best timing resolutions obtained in this experiment. Four events were found to exhibit a CsI scintillator fit error under 0.1 ns in at least one channel. These findings are summarized in Tab. V and the CsI channel data giving the smallest observed uncertainty, 0.0833 ns, is given in Fig. 12. These results demonstrate that the goal time resolution of 0.1 ns can be readily achieved for high energy particles.

B. High energy events

V. CONCLUSION

In this experiment we have assembled a cosmic muon stack detector and successfully measured muons passing through. Caesium iodide crystal scintillators with assoicated Gaussian filter measurement systems have been tested and the design time resolution of 0.1 ns was ob-

served. More work needs to be carried out, however, to understand events woth an anomalous timing sequence.

Several improvements could be implemented for future iterations of the stack detector. Firstly, a controlled calibration system could be implemented. A high energy laser would be ideal although potentially difficult to obtain. Secondly. the trigger system could be refined to reduce null triggers. The trigger area should cover the CsI are more tightly. A third trigger to reduce accidental could also be installed. Thirdly, the multi-wire chambers could be improved, or more likely, completely replaced. Larger wire chambers that cover, and are efficient, over the full CsI area would be ideal. They could also be upgraded to drift chambers for improved spatial resolution if desired. Lastly, an investigation into possible backgrounds could be carried out and measures. If extending the run time of the experiment significantly past 10,000 events, more efficient code for the first steps of the data analysis may need to be written.

[1] **E14** Collaboration, T. Yamanaka *et al.*, "Proposal for $K_L^0 \to pi^0\,\nu\,\overline{\nu}$ experiment at J-Parc,". `http://hep.uchicago.edu/cpv/e14proposal.pdf`.

[2] N. Cabibbo, "Unitary symmetry and leptonic decays," *Phys. Rev. Lett.* **10** (Jun, 1963) 531–533.

[3] M. Kobayashi and T. Maskawa, "*cp*-violation in the renormalizable theory of weak interaction," *Progress of Theoretical Physics* **49** no. 2, (1973) 652–657.

[4] L. S. Littenberg, "*CP*-violating decay $K_L^0 \to \pi^0\,\nu\,\overline{\nu}$," *Phys. Rev. D* **39** (Jun, 1989) 3322–3324.

[5] **E391a** Collaboration, J. K. Ahn *et al.*, "Experimental study of the decay $K_L^0 \to \pi^0\,\nu\,\overline{\nu}$," *Phys. Rev. D* **81** (Apr, 2010) 072004, `arXiv:0911.4789v2 [hep-ex]`.

[6] **E731** Collaboration, G. Graham *et al.*, "Search for the decay $K_L \to \pi^0\,\nu\,\overline{\nu}$," *Physics Letters B* **295** no. 1-2, (1992) 169 – 173.

[7] **E799** Collaboration, M. Weaver *et al.*, "Limit on the branching ratio of $K_L \to \pi^0\,\nu\,\overline{\nu}$," *Phys. Rev. Lett.* **72** (Jun, 1994) 3758–3761.

[8] **kTeV** Collaboration, J. Adams *et al.*, "Search for the decay $K_L \to \pi^0\,\nu\,\overline{\nu}$," *Physics Letters B* **447** no. 3-4, (1999) 240 – 245, `arXiv:hep-ex/9806007v2`.

[9] **E799** Collaboration, A. Alavi-Harati *et al.*, "Search for the decay $K_L \to \pi^0\,\nu\,\overline{\nu}$ using $\pi^0 \to e^+\,e^-\,\gamma$," *Phys. Rev. D* **61** (Mar, 2000) 072006, `arXiv:hep-ex/9907014v1`.

[10] **E391** Collaboration, J. K. Ahn *et al.*, "New limit on the $K_L^0 \to \pi^0\,\nu\,\overline{\nu}$ decay rate," *Phys. Rev. D* **74** (Sep, 2006) 051105, `arXiv:hep-ex/0607016v2`.

[11] **KEK** Collaboration, J. K. Ahn *et al.*, "Search for the decay $K_L^0 \to \pi^0\,\nu\,\overline{\nu}$," *Phys. Rev. Lett.* **100** (May, 2008) 201802, `arXiv:0712.4164v2 [hep-ex]`.

[12] G. Charpak, "Evolution of the automatic spark chambers," *Annual Review of Nuclear Science* **20** no. 1, (1970) 195–254.

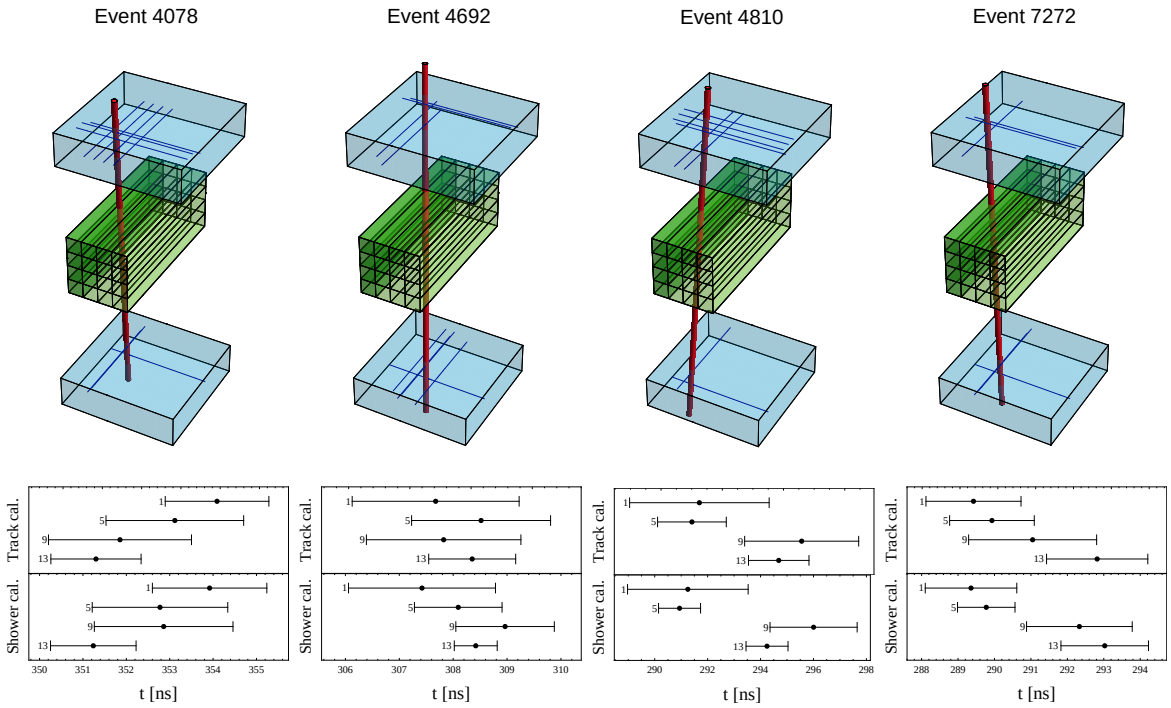

FIG. 13. All reconstructed events through CsI column 1, 5, 9, 13. (Figure for computer viewing only)

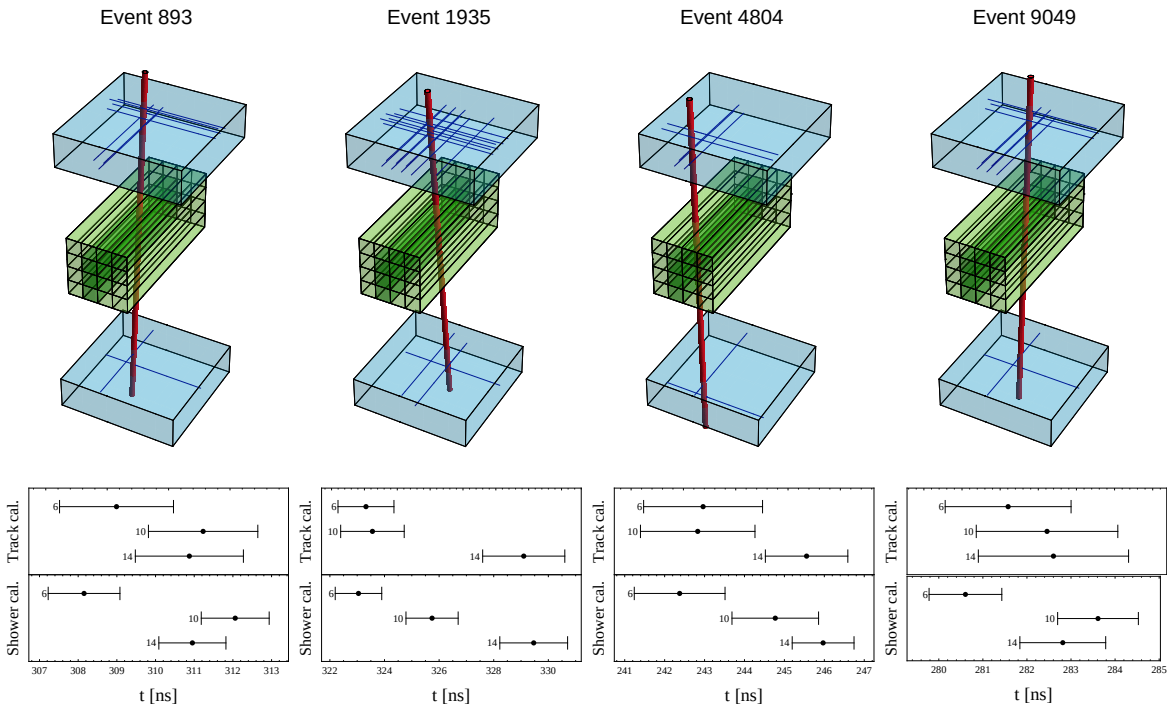

FIG. 14. Random selection of reconstructed events through CsI column 6, 10, 14. (Figure for computer viewing only)

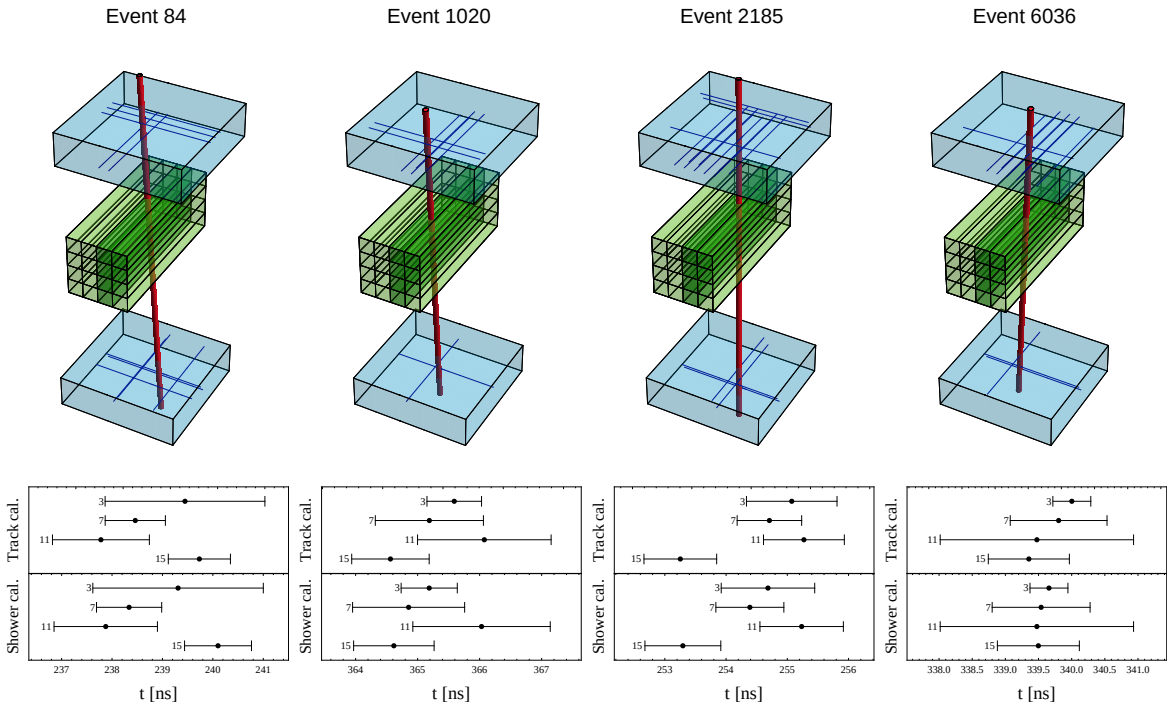

FIG. 15. Random selection of reconstructed events through CsI column 3, 7, 11, 15. (Figure for computer viewing only)

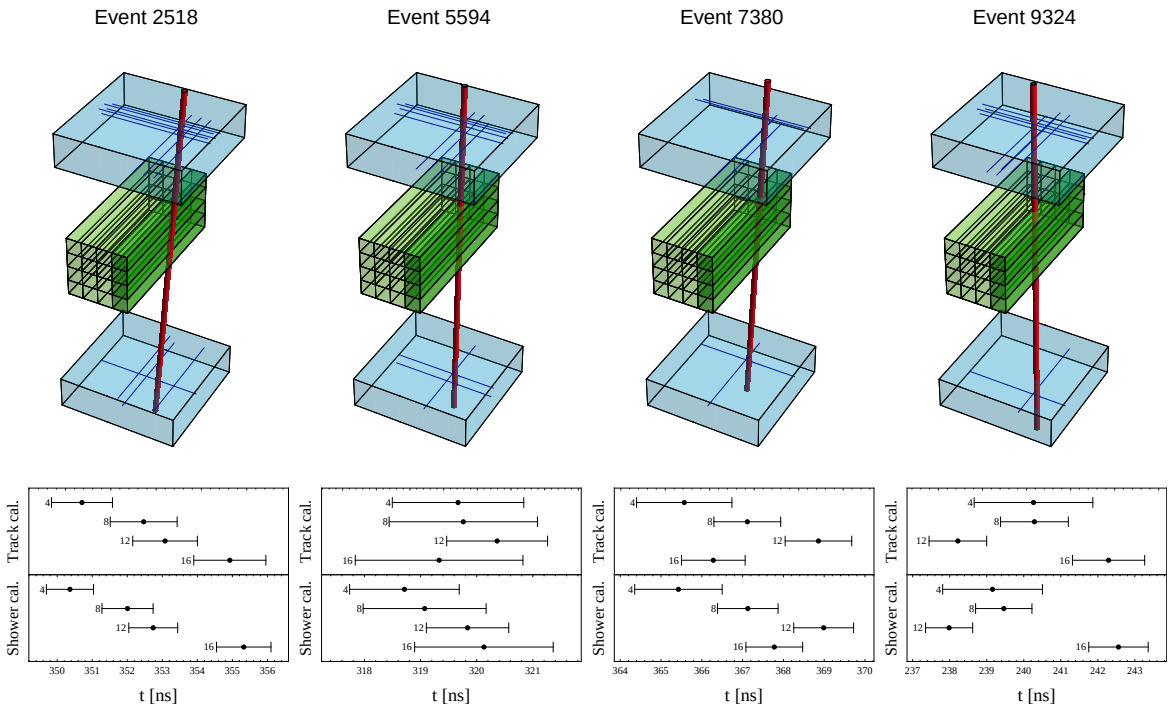

FIG. 16. Random selection of reconstructed events through CsI column 4, 8, 12, 16. (Figure for computer viewing only)